Journal of Molecular Structure 1274P1 (2023) 134496

Contents lists available at ScienceDirect

Journal of Molecular Structure

journal homepage: www.elsevier.com/locate/molstr

Effects of external fields on the nonlinear optical rectification and second harmonic generation of GaAs/GaAlAs zigzag quantum well

A.Turker Tuzemen[a,*], H. Dakhlaoui[b,c], F. Ungan[d]

[a] Department of Mathematics and Science Education, Faculty of Education, Sivas Cumhuriyet University, 58140, Sivas, Turkey
[b] Nanomaterials Technology unit, Basic and Applied Scientific Research Center (BASRC), College of Science of Dammam, Imam Abdulrahman Bin Faisal University, P. O. Box 1982, 31441 Dammam, Saudi Arabia
[c] Department of Physics, College of Sciences for Girls, Imam Abdulrahman Bin Faisal University, Dammam, Saudi Arabia
[d] Department of Physics, Faculty of Science, Sivas Cumhuriyet University, 58140, Sivas, Turkey

ARTICLE INFO

Article history:
Received 3 October 2022
Revised 1 November 2022
Accepted 4 November 2022
Available online 6 November 2022

Keywords:
Zigzag quantum well
Nonlinear optical rectification
Second harmonic generation
Electric and magnetic fields

ABSTRACT

For the first time, the impact of externally applied static electric and magnetic field on the nonlinear optical rectification (NOR) and second harmonic generation (SHG) coefficients of GaAs/GaAlAs zigzag quantum well is theoretically investigated in this study. Additionally, we examined the effect of physical parameters such as width and depth of the structure on these coefficients. We have numerically solved the time-independent Schrödinger equation by using the diagonalization method under the effective mass approximation for obtaining subband energy levels and wave functions of the structure, and then we have used the compact density matrix method to obtain the analytical expressions of NOR and SHG coefficients. The obtained numerical results showed that when the magnitude of the externally applied electric and magnetic fields is increased, the peak position of NOR and SHG shifts to blue, and by increasing the width and potential depth of the quantum well, it shifts to red.

1. Introduction

Recently, different electronic and optoelectronic devices are designed and manufactured owing to developing growth technologies like molecular beam epitaxy (MBE) and metal-organic chemical vapor deposition (MOCVD). Studies on this subject also speed up the experimental and theoretical research on low dimensional semiconductor heterostructures such as quantum wells (QWs), quantum well wires (QWWs), and quantum dots (QDs). Today, these heterostructures present a wide range of potential applications for electronic and optoelectronic devices [1,2]. These application areas can be classified as infrared lasers [3], infrared photodetectors [4], optical switches [5], high-speed electro-optical modulators [1], etc. The most intensively studied low dimensional heterostructures are QWs because of their remarkable properties. The QW structures have different shapes such as square QW [6, 7], parabolic QW [8, 9], semi parabolic QW [10, 11], graded QW [12], etc. can be formed by using the aforementioned growth techniques. The electrical and optical properties of QWs structures can be affected by various parameters like potential profile's shape, QW's width, barrier's height, number of QWs significantly. In addition to these parameters, external fields applied to the QW structure such as intense laser, electric and magnetic fields are other important factors that change the electric and optical properties of the structure. Lots of studies have been done related to optical absorption coefficients (OACs) and refractive index changes (RICs) [13–17], nonlinear optical rectification (NOR), second harmonic generation (SHG), and third harmonic generation (THG) [18–22] in the QW structures under external fields. Kasapoglu et al. have investigated the OACs and RICs in the step-like QW structure under the effects of electric and magnetic fields and showed that electric and magnetic fields caused shifting to blue shift in OACs and RICs [13]. Al et al. have studied the electric and magnetic fields' combined effects on the OACs and RICs in the $GaAs/Ga_{1-x}Al_xAs$ QWs which had asymmetric double inverse parabolic structure and determined that the OACs and RICs were sensitive to electric and magnetic fields' change with the parameters of the structure [14]. Özbakır has searched the variations of the OACs and the RICs by analyzing the transition between the ground and first excited states in the GaAs/GaAlAs QW under electric and tilted magnetic field and has shown that the applied external fields affected the system's optical properties [15]. For the asymmetric GaAs/GaAlAs double quantum well structure, how the electric and magnetic fields change affects the linear and third-order nonlinear OACs and RICs under intense laser field, has

* Corresponding author.
E-mail address: atuzemen@cumhuriyet.edu.tr (A. Tuzemen).

https://doi.org/10.1016/j.molstruc.2022.134496
0022-2860/

been examined by Yesilgul et al. In the obtained results, it has been seen that while the peak positions of the OACs and the RRICs shifts blue by increasing the magnitude of electric and magnetic fields, the peak positions shift blue first and then red respectively with increasing the intense laser field [16]. Ozturk and Sökmen studied the intersubband OACs and the RRICs in the triple QW which has different well structures by changing the width of the barrier. They showed that the changes in the barrier width affected the intersubband transitions and the energy levels in discussed structure [17]. Martinez-Orozco et al. have investigated nonlinear optical properties of the GaAs delta-doped field-effect transistor systems under different hydrostatic pressures [18]. They have found a hydrostatic pressure interval where the nonlinear optical rectification and second harmonic generation resonant peaks' amplitude were enhanced. They have also proved that for the third-harmonic generation (THG), the best scenario has appeared at the zero value of the pressure. For a semi-parabolic typical GaAs/$Ga_{1-x}Al_xAs$ QW under the effect of the intense laser field, Ungan et al. have investigated the NOR and SHG coefficients about the intersubband transitions by changing electric and magnetic fields. They have determined the effects of mentioned external fields on the resonant peak energy positions and magnitude of the coefficients [19]. In another study, Ozturk et al. have examined two different QW structures such as square-step QWs and graded-step QWs and determined the changes in the NOR, SHG, and THG coefficients for different values of the intense laser field. Their results have shown that the effect of intense laser field on the potential height and profile for graded-step QWs were more important than the effect on square-step QWs and the NOR, SHG, and THG coefficients of both QW structures might have been set to desired energy range and the resonance peak's magnitude by applied intense laser field [20]. The NOR, SHG, and THG calculations under the electric, magnetic intense laser fields have been done for a GaAs QW which had asymmetrical Gaussian potential by Sayrac et al. As a result of their calculations, they have observed that changing of the external fields caused changes in these values of the structure [21]. In his work, Altuntas has studied GaAs/GaAlAs QW with exponentially confinement potential and calculated the NOR, SHG, and THG coefficients of the system for different values of applied external fields (electric, magnetic, and non-resonant intense laser fields). He has obtained that the optical properties of the handled system were affected greatly by the external fields [22]. In another study, Aydinoglu et al. have interested $Al_xGa_{1-x}As$/GaAs asymmetric double graded QWs and examined the effect of external fields such as electric and magnetic and changing parameters of the structures on the NOR, SHG, and THG coefficients [23]. In addition to these studies on quantum wells, some of the studies on quantum dot structures are as follows. Pal and Ghosh [24] have studied the effect of Gaussian white noise on the nonlinear optical rectification (NOR) coefficients of doped quantum dot (QD) and determined that the NOR profiles sensitively affected by application of the noise. In addition to this, second harmonic generation (SHG) coefficient of impurity-doped quantum dots (QDs) in presence and absence of noise has been examined by Ganguly and Ghosh [25] and it has been determined that the properties of SHG profiles has changed with the effect of noise. Ganguly et al. [26] has investigated that how the combined effect of hydrostatic pressure and temperature in absence and presence of Gaussian white noise changed the optical rectification (OR), second harmonic generation (SHG) and third harmonic generation (THG) for impurity doped QD structure. They showed that changes in temperature and pressure created shift (blue/red) of the peaks of nonlinear optical properties and a change in the peak heights (increase/decrease). In another study, Arif et al. [27] has analysed the role of relaxation time on second harmonic generation (SHG) of doped quantum dot (QD) and they put forth that SHG peak values had a monotonic behavior with change of relaxation time.

We presented theoretically the changes formed in the NOR and SHG coefficients because of the different applied external electric and magnetic fields for GaAs/GaAlAs zigzag QW structure in this work. In addition, we examined the changes in the NOR and SHG coefficients depending on the parameters as the depth (V_0) and the width (L_w) of the structure. Our article's organization has been done as follows: the problem's definition and solution theoretically are given in part 2, obtained numerical results are given in part 3, discussions of the numerical results, and our conclusions are presented in part 4.

2. Theory

In our study, we assume a zigzag QW structure (shown in Fig. 1) which is grown in the z-direction. While applied electric field's direction is taken as the growth direction ($\vec{F}=F\hat{z}$), the magnetic field is considered perpendicular to the growth direction ($\vec{B}=B\hat{x}$). We examined the effects of these applied electric and magnetic fields on NOR and SHG coefficients' changes. Under applied external fields, the total Hamiltonian for an electron which is confined in the zigzag QWs is written by

$$H=\frac{1}{2m^*}\left[\vec{p}+\frac{e}{c}\vec{A}\right]^2+V(z)+eFz \tag{1}$$

here m^*, $\vec{p}$ and e are the effective mass, the momentum operator, and the charge of the confined electron respectively. c is the velocity of light and $\vec{A}=\vec{A}(\vec{r})$ is the magnetic vector potential. Confined potential of the zigzag QWs is identified as $V(z)$ and expressed as

$$V(z)=\begin{cases} V_0 & z<-\frac{3L_w}{2} \\ \left(\frac{z+3L_w/2}{L_w}\right)V_0 & -\frac{3L_w}{2}<z<-\frac{L_w}{2} \\ \left(\frac{z+L_w/2}{L_w}\right)V_0 & -\frac{L_w}{2}<z<\frac{L_w}{2} \\ \left(\frac{z-L_w/2}{L_w}\right)V_0 & \frac{L_w}{2}<z<\frac{3L_w}{2} \\ V_0 & z>\frac{3L_w}{2} \end{cases} \tag{2}$$

in these expressions, V_0 and L_w show the depth and the width of the structure respectively.

If the time-independent Schrödinger equation along the growth-direction in one dimension is written, the expression below is obtained [8],

$$\left[-\frac{\hbar^2}{2m^*}\frac{d^2}{dz^2}+\frac{e^2B^2z^2}{2m^*c^2}+V(z)+eFz\right]\psi(z)=E\psi(z) \tag{3}$$

E and $\psi(z)$ state the energy levels and wave functions of the structure respectively under the applied external fields in this equality.

We solved Eq. (3) numerically by using diagonalization method to find out energy eigen values and wave functions of the structure [28]. After that, we have used the compact density matrix method to obtain the analytical expressions of the NOR and SHG coefficients [29, 30]. Obtained NOR and SHG coefficients are given below respectively,

$$\chi_0^{(2)}=\frac{4e^3\rho_\upsilon}{\varepsilon_0\hbar^2}M_{01}^2\delta_{01}\frac{\omega_{01}^2(1+\Gamma_2/\Gamma_1)+\left(\omega^2+\Gamma_2^2\right)(\Gamma_2/\Gamma_1-1)}{\left[(\omega_{01}-\omega)^2+\Gamma_2^2\right]\left[(\omega_{01}+\omega)^2+\Gamma_2^2\right]} \tag{4}$$

$$\chi_{2\omega}^{(2)}=\frac{e^3\rho_\upsilon}{\varepsilon_0\hbar^2}\frac{M_{01}M_{12}M_{20}}{(\omega-\omega_{10}-i\Gamma_3)(2\omega-\omega_{20}-i\Gamma_3)} \tag{5}$$

In the Eqs. (4) and (5), M_{ij} represent the dipole matrix elements ($M_{ij} = |\langle\varphi_i|ez|\varphi_j\rangle|$, $(i,\ j = 0,\ 1,\ 2)$ and $\delta_{01} = |M_{00} - M_{11}|$). The transition frequency is given by the equation $\omega_{ij} = (E_i - E_j)/\hbar$. ρ_υ and ε_0 show the electronic density and permittivity of vacuum, respectively. Γ_k equals $1/T_k$ $(k = 1,\ 2,\ 3)$ and it defines relaxation rate associated with the electrons' transition lifetime.

3. Results and discussion

In our study, we took the depth and the width of the zigzag QWs as $V_0 = 270\ meV$, $L_w = 70$ Å. In addition, the numerical values of the physical expressions used in this article: $m^* = 0.067m_0$ (where m_0 is the free electron mass), $\varepsilon = 12.58$, $\varepsilon_0 = 8.854 \times 10^{-12}$, $e = 1.602 \times 10^{-19}C$, $\hbar = 1.056 \times 10^{-34}$Js, $\rho_\upsilon = 3 \times 10^{22}m^{-3}$, $\Gamma_k = (k = 1, 2, 3)$ is 1, 5 and 7 THz, respectively.

The changes in the confining potential and the probability density for the envelope wave-functions of the ground state, first and second excited states due to the applied external fields are indicated in Fig. 1 for $V_0 = 270\ meV$ and $L_w = 70$ Å. When both electric and magnetic fields are zero, there are probability concerning are approximately symmetrical with respect to the center of the heterostructure (Fig. 1(a)). The ground state, first excited state and second excited state have one peak (in the middle well), two peaks (in the right and the left well) and three peaks (in each well) respectively. In the first case we took the value of the electric field which had the same direction with the heterostructure's growth as 40 kV/cm under zero magnetic field (Fig. 1(a)). Applied electric field changes the shape of the confinement potential compared to the case $F = 0$. The left side of confinement potential is bent seriously because of the electric field's effect. Besides, the symmetries (approximately) in the electron's localization are damaged for all states. In the ground state, the electron's localization increases in the left well, while it decreases for the other wells. For the first and second excited states, electron's localizations increase in the middle and the right wells respectively.

We examined the case where applied magnetic field which was perpendicular to the growth's direction in Fig. 1(b) for $F = 0$, $V_0 = 270\ meV$ and $L_w = 70$ Å conditions. In the case of magnetic and electric fields are zero, the probability densities were approximately symmetrical with respect to the structure's center as stated above. Because of the parabolic term (z^2) in Schrödinger equation which comes from the effect of the magnetic field, the upper part of the confinement potential takes a parabolic shape near the edges of the structure and almost unchanged near the center. The distributions of the wave functions are almost the same as in the case of $B = 0$ due to symmetry of the confining potential. Additionally, the increase in E_1 and E_2 is slightly greater than the increase in E_0 due to the fact that the ground wavefunction is more confined than the excited ones. However, the impact of the electric field is clearly noticed, in fact, as seen in Fig. 1(a), the energy level of the ground state rises considerably and its wavefunction is moved to the left triangular quantum well.

As a conclusion from the investigation showed in Figs. 1(a) and (b), it can be said that the symmetries in the electron's localization in all analyzed states are changed only in the presence of the electric field, but they remain almost the same in the presence of the magnetic field.

Fig. 2 shows the graphs included nonlinear optical rectification coefficient as a function of incident photon energy for different values of the width (L_w) and the depth (V_0) of the heterostructure in the absence of the applied external fields respectively. In Fig. 2(a) while the depth of the heterostructure V_0 is taken as 270 meV, different values of the heterostructure's width L_w are used as 60 Å, 70 Å and 80 Å. The NOR peak position and the peak amplitude have been affected by changing the well width. As the well width increases, the NOR peak amplitude increases and the NOR peak position shifts to low energy region (redshift). This shift towards low energies is attributed to the reduction of the energy interval between the E_1 and E_0.

The depth's values of the heterostructure V_0 are changed as 228 meV, 270 meV and 312 meV in the case of L_w equals 70 Å in Fig. 2(b). While the well depth increases, the NOR peak amplitude increases slightly and the position of the NOR peak has redshift. In both cases in Figs. 2(a) and 2(b), as the values of the well width and depth increases the NOR peak positions show redshift. But the effect of changing the well width on NOR peak position and peak amplitude is stronger than the effect of the well depth change. Numerical values of the electron subband energy differences and dipole moment matrix elements are presented in Table 1 in the cases of the increasing well width and depth. Decreasing in electron subband energy difference with increasing well width is faster compared to the case with increasing well depth. Similarly, if the changes in dipole moment matrix elements are examined, it can be seen that increasing in the values of the matrix elements is faster in the case of increasing of L_w.

Nonlinear optical rectification coefficients are redrawn as a function of incident photon energies for different values of the applied electric and magnetic fields in Fig. 3. V_0 and L_w values are taken as 270 meV and 70 Å respectively in these figures. The values of applied electric field are changed as 0, 20 kV/cm and 40 kV/cm

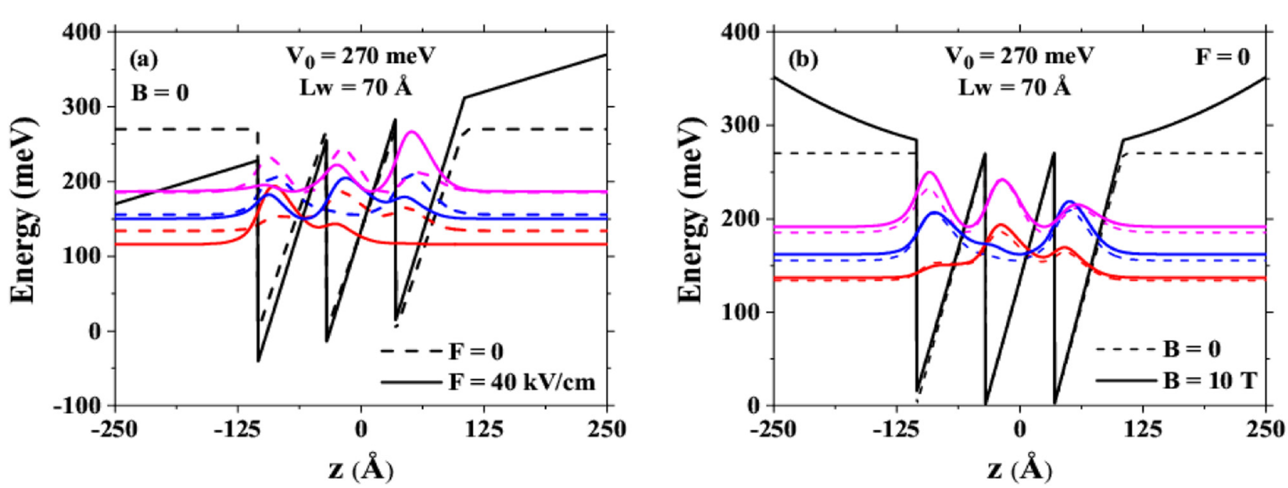

Fig. 1. The changes occurred in the confinement potential and the probability density for the envelope wave-functions of the ground, first and second excited states for $V_0 = 270\ meV$ and $L_w = 70$ Å in the presence of the (a) electric field, (b) magnetic field.

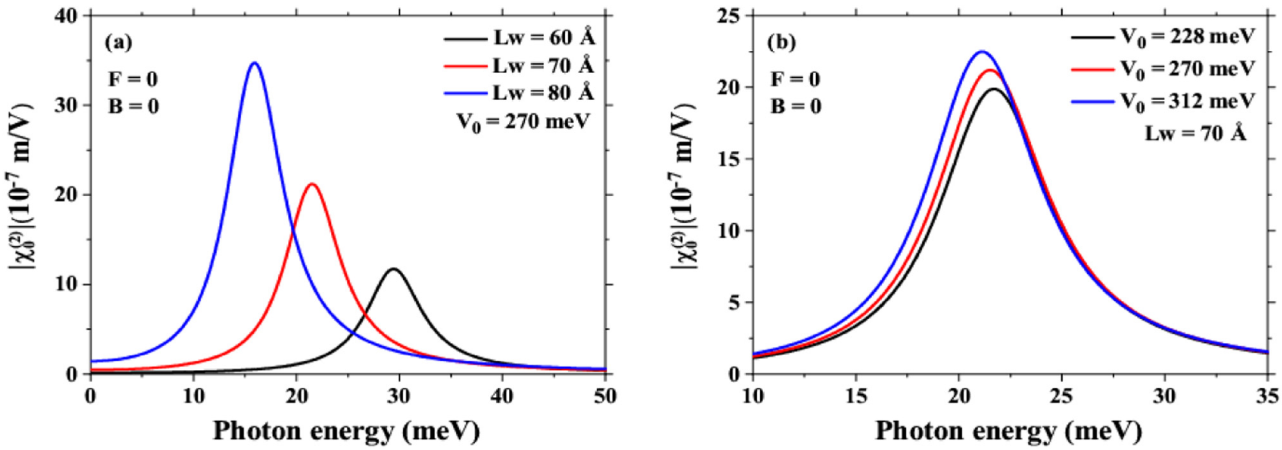

Fig. 2. Nonlinear optical rectification coefficient as a function of incident photon energy in zigzag QW in the absence of applied external fields for different values of (a) the width (L_w) and (b) the depth (V_0) of the structure.

Table 1
Numerical values of the electron subband energy differences and dipole moment matrix elements for different values of (a) the width (L_w) and (b) the depth (V_0) of the well.

L_w(Å)	$(E_1 - E_0)$ (meV)	$(E_2 - E_0)/2$ (meV)	$M_{01}^2\delta_{01}$(Å^3)	$M_{01}M_{12}M_{20}$(Å^3)
60	29.9337	36.4935	4466,76	57.1552
70	21.39	25.705	8027.98	344.192
80	15.757	18.1135	13,005.9	1211.22
$\boldsymbol{V(z)}$ $(\boldsymbol{meV})$				
228	21.576	26.4885	7528.82	107.83
270	21.39	25.705	8027.98	344.192
312	21.001	24.6895	8511.17	555.652

under zero magnetic field in Fig. 3(a). Applying the electric field to zigzag QW increases the difference between electron energies which confirms the result observed in Fig 1(a). The positions of resonance peak of NOR coefficients also display a blue-shift due to the increase in the energy differences between ground and first excited states $(E_1 - E_0)$. The magnitude of peak increases when the value of the applied electric field is changed from 0 to 20 kV/cm firstly. After that it shows decreasing behavior when the electric field reaches the value of 40 kV/cm. The reason of this result can be seen from Table 2. While there is a small increase in the difference between E_0 and E_1 when F value is changed from 0 to 20 kV/cm, the increase in this difference happens bigger for F value changing from 20 kV/cm to 40 kV/cm. While there is a substantial increase in the change in the $M_{01}^2\delta_{01}$'s value for F value changing from 0 to 20 kV/cm, the value of $M_{01}^2\delta_{01}$ shows a small decrease compared to the previous case when F value changing from 20 kV/cm to 40 kV/cm. As a result of these changes in $(E_1 - E_0)$ and $M_{01}^2\delta_{01}$ the magnitude of NOR peak shows a significant increase firstly, and then a small decrease.

In Fig. 3(b) the applied magnetic field takes the values 0, 10 T and 20 T in the absence of the electric field. As in the case of increasing the applied electric field in Fig. 3(a) a blueward shift is observed in the NOR coefficients peak positions. Here, the increase in the position of the peak is small as the magnetic field is in-

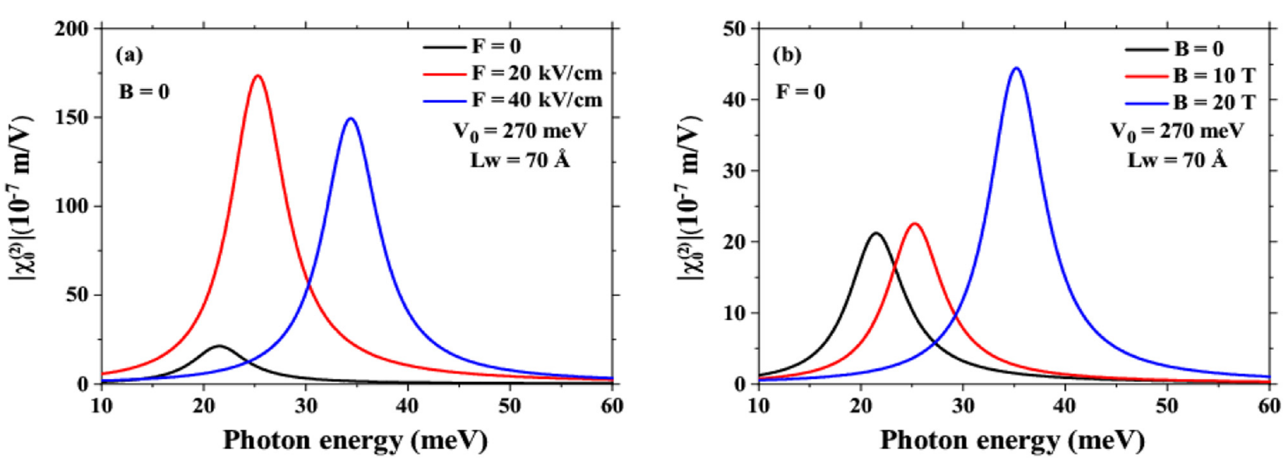

Fig. 3. Nonlinear optical rectification coefficient as a function of incident photon energy in zigzag QW under different values of the (a) applied electric field (F) in the absence of the applied magnetic field ($B = 0$) and (b) applied magnetic field (B) in the absence of the applied electric field ($F = 0$).

Table 2
Numerical values of the electron subband energy differences and dipole moment matrix elements for different values of the applied (a) electric field (F) and (b) magnetic field (B).

F (kV/cm)	$(E_1 - E_0)$ (meV)	$(E_2 - E_0)/2$ (meV)	$M_{01}^2\delta_{01}(\text{Å}^3)$	$M_{01}M_{12}M_{20}(\text{Å}^3)$
0	21.39	25.705	8027.98	344.192
20	25.197	27.8385	65,931.8	10,825.3
40	34.316	35.446	57,042.9	7850.73
***B* (*T*)**				
0	21.39	25.705	8027.98	344.192
10	25.164	27.3635	8571.36	756.07
20	35.138	34.9815	16,971.3	6241.7

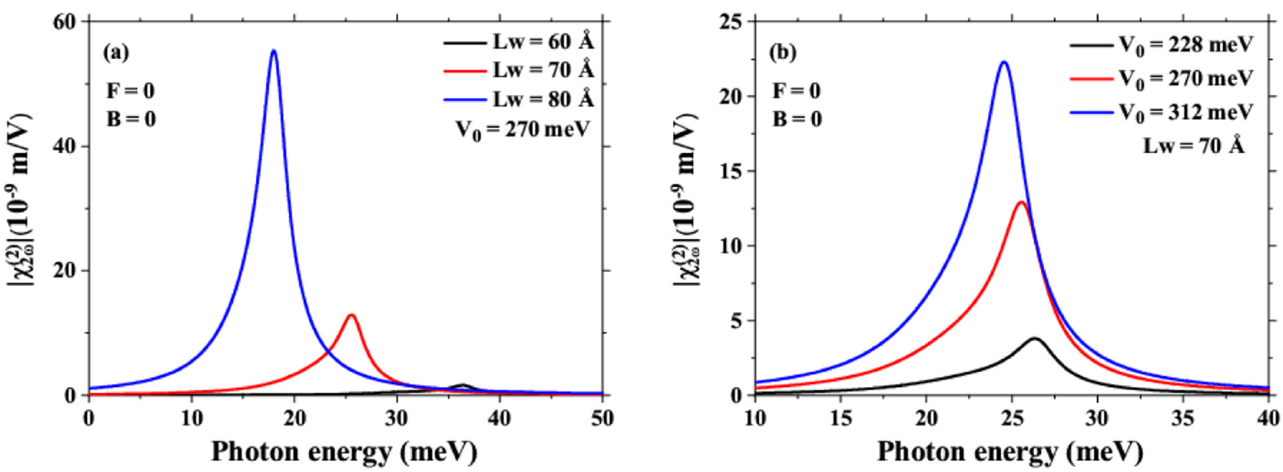

Fig. 4. Second harmonics generation coefficient as a function of incident photon energy in zigzag QW under zero values of the external fields for different values of (a) the width (L_w) and (b) the depth (V_0) of the structure.

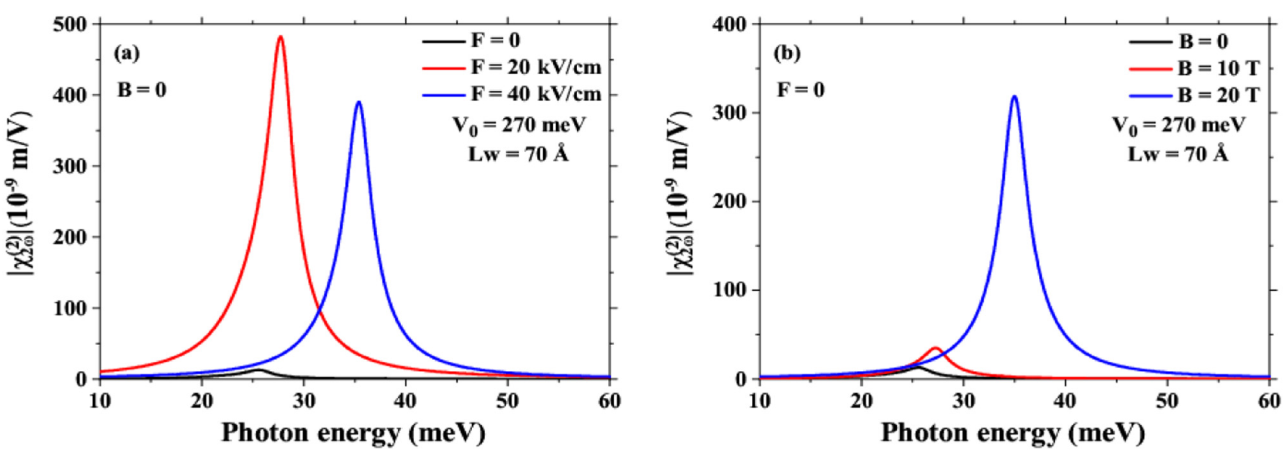

Fig. 5. Second harmonics generation coefficient as a function of incident photon energy in zigzag QW under different values of the (a) applied electric field (F) in the case of the zero magnetic field ($B = 0$) and (b) applied magnetic field (B) in the case of the zero electric field ($F = 0$).

creased from 0 to 10 T (small increase in the difference between E_0 and E_1). When B is increased to 20 T, peak position shows a larger increase than the first case (big increase in the difference between E_0 and E_1). When Table 2 is examined, it can be seen that the values of dipole matrix elements ($M_{01}^2\delta_{01}$) show a small increase (between 0 and 10 T) and a much bigger increase (between 10 T and 20 T) respectively. The changes in the position of the NOR's peak are happened depending on changing in the difference between ground-first excited states and in the values of dipole matrix elements.

The changes of the second harmonics generation coefficients against incident photon energy are given in Fig. 4 under the same conditions in Fig. 2. Obtained results from this investigation are consistent with the results found out for Fig. 2. Both the cases of the increasing well width and depth the SHG coefficients are affected and the SHG peak positions shift to lower energy region (redshift) with increasing peak amplitudes. The numerical values of the SHG coefficients ($M_{01}M_{12}M_{20}$) and subband energy differences ($(E_2 - E_1)/2$) related to Figs. 4(a) and 4(b) are given in Table 1. As it can be understood from the data in the table, the changing of the width of the well is more effective on the values of the SHG coefficients than the well depth's changing.

In the last part of the study, SHG coefficients have been obtained as a function of incident photon energies for the same conditions in Fig. 3 under different magnitudes of the electric and the magnetic fields. The SHG coefficients peak's positions show a blue-shift due to the increase in the energy differences between ground and second excited states ($E_2 - E_0$). The peak's magnitude increases firstly in the case of the value of F changed from 0 to 20 kV/cm and then it decreases when electric field takes the value of the 40 kV/cm (Fig. 5(a)). Table 2 shows that the changes in ($E_2 - E_0$) and ($M_{01}M_{12}M_{20}$) explain that the SHG peak's magnitude increases significantly at first, and then decreases by a small amount.

In Fig. 5(b) the effects of the changes in the applied magnetic field on SHG coefficients are examined. In this situation it is also observed a blueshift as in Fig. 5(a). There is a small increase in peak's position for magnetic field's change from 0 to 10 T (small increase in the difference between E_0 and E_2). When magnetic field increase to 20 T, peak position increases more than before (big increase in the difference between E_0 and E_2). It is given that the values of dipole matrix elements $M_{01}M_{12}M_{20}$ increases by a small amount (between 0 - 10 T) and increases largely (between 10 T and 20 T) in Table 2 respectively.

4. Conclusion

In this work, we have investigated the changes in the nonlinear optical rectification and second harmonic generation coefficients in GaAs/GaAlAs zigzag quantum well under different external fields like electric and magnetic theoretically. Furthermore, we have examined the effects of the well width and depth on these coefficients. We have used diagonalization method for numerically solving Schrödinger equation and effective mass approximation for obtaining energy levels and wave functions of the structure. The analytical expressions of NOR and SHG coefficients have been obtained from the compact density matrix method. The investigations proved that the applied electric and magnetic fields affect the NOR and the SHG coefficients. The resonant peaks of the nonlinear optical rectification and second harmonic generation coefficients shift to higher energies (blue shift) under the applied electric and magnetic fields' increments. Furthermore, the impact of the electric field on the NOR and the SHG coefficients was more pronounced than that of the magnetic field due to the fact that the electric field breaks considerably the symmetry of the structure, while the magnetic one conserves it. At the same time, these resonant peaks shift to lower energies (red shift) with the effect of increase in width and depth of the well. These findings in the optical properties of GaAs/GaAlAs zigzag quantum wells in the presence of external fields may provide guidance to practical studies, especially in designing new optoelectronic devices operating under the action of external fields.

Declaration of Competing Interest

The authors do not have any financial and non-financial competing interest statement.

Data availability

Data will be made available on request.

Acknowledgement

This research did not receive any specific grant from funding agencies in the public, commercial, or not-for-profit sectors.

References

[1] E. Leobandung, L. Guo, S.Y. Chou, Single hole quantum dot transistors in silicon, Appl. Phys. Lett. 67 (1995) 2338, doi:10.1063/1.114337.

[2] X. Jiang, S.S. Li, M.Z. Tidrow, Study of intersubband transition in quantum dots and quantum dot infrared photodetectors, Physica E 5 (1999) 27–35, doi:10.1016/S1386-9477(99)00026-0.

[3] K. Imamura, Y. Sugiyama, Y. Nakata, S. Muto, N. Yokoyama, New optical memory structure using self-assembled InAs quantum dots, Jpn. J. Appl. Phys. 34 (1995) L 1445, doi:10.1143/JJAP.34.L1445.

[4] F. Durante, P. Alves, G. Karunasiri, N. Hanson, M. Byloos, H.C. Liu, A. Bezinger, M. Buchanan, NIR, MWIR and LWIR quantum well infrared photodetector using interband and intersubband transitions, Infrared Phys. Tech. 50 (2007) 182–186, doi:10.1016/j.infrared.2006.10.021.

[5] S.A.-B. Nasrallah, N. Sfina, M. Said, Electronic properties of intersubband transition in (CdS/ZnSe)/BeTe quantum wells, Eur. Phys. J. B 47 (2005) 167–170, doi:10.1140/epjb/e2005-00323-0.

[6] F. Ungan, U. Yesilgul, E. Kasapoglu, H. Sari, I. Sökmen, The effects of hydrostatic pressure and intense laser field on the linear and nonlinear optical properties of a square quantum well, Opt. Commun. 285 (2012) 373–377, doi:10.1016/j.optcom.2011.09.060.

[7] P.A. Belov, Calculation of energy states of excitons in square quantum wells, Semiconductors 52 (2018) 551–553, doi:10.1134/S1063782618050032.

[8] U. Yesilgul, F. Ungan, S. Sakiroglu, M.E. Mora-Ramos, C.A. Duque, E. Kasapoglu, H. Sarı, I. Sökmen, Effect of intense high-frequency laser field on the linear and nonlinear intersubband optical absorption coefficients and refractive index changes in a parabolic quantum well under the applied electric field, J. Luminescence 145 (2014) 379–386, doi:10.1016/j.jlumin.2013.07.062.

[9] H. Dakhlaoui, F. Ungan, J.C. Martínez-Orozco, M.E. Mora-Ramos, Theoretical investigation of linear and nonlinear optical properties in an heterostructure based on triple parabolic barriers: Effects of external fields, Physica B 607 (2021) 412782, doi:10.1016/j.physb.2020.412782.

[10] E. Ozturk, Electric and intense laser field effect on the electronic properties of $Ga_{1-x}Al_xAs$/GaAs and $Ga_{1-x}In_xAs$/GaAs semi-parabolic quantum wells, Laser Phys. 26 (2016) 096102, doi:10.1088/1054-660X/26/9/096102.

[11] E. Kasapoglu, C.A. Duque, H. Sari, I. Sökmen, Intense laser field effects on the linear and nonlinear intersubband optical properties of a semi-parabolic quantum well, Eur. Phys. J. B 82 (2011) 13–17, doi:10.1140/epjb/e2011-20243-6.

[12] H.S. Aydinoglu, S. Sakiroglu, H. Sari, F. Ungan, I. Sökmen, Nonlinear optical properties of asymmetric double-graded quantum wells, Philos. Mag. 98 (23) (2018) 2151–2163, doi:10.1080/14786435.2018.1476785.

[13] E. Kasapoglu, F. Ungan, C.A. Duque, U. Yesilgul, M.E. Mora-Ramos, H. Sari, I. Sokmen, The effects of the electric and magnetic fields on the nonlinear optical properties in the step-like asymmetric quantum well, Physica E 61 (2014) 107–110, doi:10.1016/j.physe.2014.03.024.

[14] E.B. Al, F. Ungan, U. Yesilgul, E. Kasapoglu, H. Sari, I. Sökmen, Effects of applied electric and magnetic fields on the nonlinear optical properties of asymmetric GaAs/$Ga_{1-x}Al_xAs$ double inverse parabolic quantum well, Opt. Mater. 47 (2015) 1–6, doi:10.1016/j.optmat.2015.06.048.

[15] R. Özbakır, Optical properties of a single quantum well under electric and tilted magnetic fields, Can. J. Phys. 96 (2018) 999–1003, doi:10.1139/cjp-2017-0384.

[16] U. Yesilgul, E.B. Al, J.C. Martínez-Orozco, R.L. Restrepo, M.E. Mora-Ramos, C.A. Duque, F. Ungan, E. Kasapoglu, Linear and nonlinear optical properties in an asymmetric double quantum well under intense laser field: Effects of applied electric and magnetic fields, Opt. Mater. 58 (2016) 107–112, doi:10.1016/j.optmat.2016.03.043.

[17] E. Ozturk, I. Sokmen, Intersubband optical absorption coefficients and refractive index changes in triple quantum well with different well shapes, Eur. Phys. J. Appl. Phys. 51 (2010) 10303, doi:10.1051/epjap/2010068.

[18] J.C. Martinez-Orozco, M.E. Mora-Ramos, C.A. Duque, Nonlinear optical rectification and second and third harmonic generation in GaAs δ-FET systems under hydrostatic pressure, J. Luminescence 132 (2012) 449–456, doi:10.1016/j.jlumin.2011.09.022.

[19] F. Ungan, J.C. Martínez-Orozco, R.L. Restrepo, M.E. Mora-Ramos, E. Kasapoglu, C.A. Duque, Nonlinear optical rectification and second-harmonic generation in a semi-parabolic quantum well under intense laser field: Effects of electric and magnetic fields, Superlattices and Microstructures 81 (2015) 26–33, doi:10.1016/j.spmi.2015.01.016.

[20] O. Ozturk, E. Ozturk, S. Elagoz, Nonlinear optical rectification, second and third harmonic generations in square-step and graded-step quantum wells under intense laser field, Chin. Phys. Lett. 36 (6) (2019) 067801, doi:10.1088/0256-307X/36/6/067801.

[21] M. Sayrac, A. Turkoglu, M.E. Mora–Ramos, F. Ungan, Intensity–dependent nonlinear optical properties in an asymmetric Gaussian potential quantum well–modulated by external fields, Optic. Quant. Electron. 53 (2021) 485, doi:10.1007/s11082-021-03136-y.

[22] I. Altuntas, Effects of applied external fields on the nonlinear optical rectification, second, and third harmonic generation in a quantum well with exponentially confinement potential, Eur. Phys. J. B 94 (2021) 177, doi:10.1140/epjb/s10051-021-00189-6.

[23] H.S. Aydinoglu, M. Sayrac, M.E. Mora-Ramos, F. Ungan, Nonlinear optical properties in $Al_xGa_{1-x}As$/GaAs double-graded quantum wells: The effect of the structure parameter, static electric, and magnetic field, Solid State Commun. 342 (2022) 114647, doi:10.1016/j.ssc.2021.114647.

[24] S. Pal, M. Ghosh, Tailoring nonlinear optical rectification coefficient of impurity doped quantum dots by invoking Gaussian white noise, Opt. Quant. Electron 48 (2016) 372, doi:10.1007/s11082-016-0640-9.
[25] J. Ganguly, M. Ghosh, Modulating optical second harmonic generation of impurity-doped quantum dots in presence of Gaussian white noise, Phys. Status Solidi B 253 (6) (2016) 1093–1103, doi:10.1002/pssb.201552606.
[26] J. Ganguly, S. Saha, A. Bera, M. Ghosh, Modulating optical rectification, second and third harmonic generation of doped quantum dots: Interplay between hydrostatic pressure, temperature and noise, Superlattices and Microstructures 98 (2016) 385–399, doi:10.1016/j.spmi.2016.08.052.
[27] S.M. Arif, A. Bera, A. Ghosh, M. Ghosh, Analyzing role of relaxation time on second harmonic generation and optical dielectric function of impurity doped quantum dots under the aegis of noise, Physica B 588 (2020) 412166, doi:10.1016/j.physb.2020.412166.
[28] E. Kasapoglu, I. Sökmen, The effects of intense laser field and electric field on intersubband absorption in a double-graded quantum well, Physica B 403 (2008) 3746–3750, doi:10.1016/j.physb.2008.06.024.
[29] E. Rosencher, P. Bois, Model system for optical nonlinearities: Asymmetric quantum wells, Phys. Rev. B 44 (20) (1991) 11315, doi:10.1103/PhysRevB.44.11315.
[30] A.S. Durmuslar, M.E. Mora-Ramos, F. Ungan, Nonlinear optical properties of n-type asymmetric double δ-doped quantum wells: role of high-frequency laser radiation, doping concentration and well width, Eur. Phys. J. Plus 135 (2020) 442, doi:10.1140/epjp/s13360-020-00465-x.